MATHEMATICA MONTISNIGRI
Vol XXXI (2014)

MOLECULAR DYNAMICS SIMULATION OF CRITICAL POINT PARAMETERS FOR SILICON

V.I. MAZHUKIN[1,2], A. V. SHAPRANOV[1,2], O.N.KOROLEVA[1,2], A.V. RUDENKO[3]

[1]Keldysh Institute of Applied Mathematics, RAS, Moscow, Russia
e-mail: vim@modhef.ru
[2] National Research Nuclear University MIPhI (Moscow Engineering Physics Institute)
Moscow, Russia
[3]Moscow Institute of Physics and Technology, State University (MIPT)
Moscow, Russia

Summary. On the basis of nine semi-empirical potentials: Stillinger-Weber (SW), Stillinger-Weber modification (SWM), Tersoff (T-C, T-D), EDIP, Erhart-Albe (EA-1, EA-2), KIHS and MIX using molecular dynamics modeling the critical parameters of silicon was determined. Analysis of simulation results and then comparing with calculations of other authors allowed us to determine the interaction potentials (EA-1, EA-2, KIHS and MIX) for which there is the greatest alignment with critical parameters of silicon used in practice.

1 INTRODUCTION

One of the fundamental problems in materials science is research of critical phenomena and determination of the critical parameters in the liquid - gas system for a wide range of pure metallic and nonmetallic materials [1,2]. Investigation of the behavior of matter in the vicinity of the critical point is a component of a more general problem - investigation of the properties of materials based on the equations of state [3-6]. However, up to the present for the vast majority elements parameters of the critical point has not been experimentally determined. The development of theoretical propositions is based on phenomenological [7, 8] and microscopic approaches [9, 10]. The use of phenomenological theory allowed us to obtain parameter estimates for a large number of elements [11]. The importance of determining the parameters of the critical point and its incompleteness are marked in [12].

During the last decades keen practical interest to critical phenomena has appeared and associated with wide application of concentrated energy flows (laser and electron beams, streams of fast particles), the power of which is sufficient to achieve near-critical and supercritical states [13,14]. In this field there are a number of unsolved problems relating to the behavior of nonequilibrium states, in particular, features of the behavior of superheated liquid phase during rapid heating of substance. Theoretical analysis of these problems can now be performed by means of mathematical modeling within the atomistic approach, in which the behavior of matter is described by molecular - dynamic (MD) models [15].

This work is devoted to the theoretical description, including determining the critical parameters such as pressure p_{cr}, density ρ_{cr} and temperature T_{cr} of silicon carried out by means of computational experiments (CEs) based on the molecular dynamics models.

2010 Mathematics Subject Classification: 82B26, 82B30, 82C27.
Key words and Phrases: Molecular dynamic, Interaction potentials, Critical parameters, Critical point, Silicon.

2 THE PROPOSED METHODS AND APPROACHES

Investigations of the behavior of matter in the vicinity of the critical point is traditionally generate an increased interest associated with a wide variety of physical properties and the unusual behavior of critical phenomena in the liquid - vapor system. Many critical phenomena experimentally were observed 50-100 years ago. From generalization of the experimental data it is known that the equation of state of condensed medium defines a surface in 3 dimensional space with coordinates: temperature T, density ρ, pressure p. Each of the points of this surface corresponds to the equilibrium state of the system. The surface projection on plane pT makes 3 separate areas corresponding to 3 aggregate states of matter: solid, liquid and gaseous. Solid and gaseous phases are in equilibrium along the curve of sublimation, solid and liquid - along the melting (hardening) curve and liquid and gaseous - along boiling (condensation) curve. Each point on these curves corresponds to the equilibrium state in which two phases can coexist. There is only one point, in which may coexist all three phases - the so-called triple point. On a plane pT the curve of sublimation from the triple point continues down to low temperatures, the melting (hardening) curve from the triple point goes to infinity, the boiling (condensation) curve in contrast to the melting curve is cut off at a certain point, called the critical point with coordinates $p_{cr}, \rho_{cr}, T_{cr}$. The fact that the boiling (condensation) curve terminates at the critical point means that the liquid (along the binodal curve) can be transformed into gas continuously without crossing the line of the phase transition, what is typical for phase transitions of the 2nd kind. The critical point is the only one point on the curve of phase equilibrium of liquid-gas - binodal, which coincides with the boundary of stability - the spinodal.

The critical state (as well as phase transitions of the second kind) on the phase equilibrium curve liquid-gas is a special singular point of the thermodynamic potential. Other points on this curve (binodal) do not consist any features of the thermodynamic potential . On the curve of phase equilibrium potentials of both phases are equal and each of them, with some reservations, can be extended into the metastable region. In the case of the critical point, the function of thermodynamic potential in a "foreign" temperature region does not correspond to any, even a metastable state. At the critical point the curve of phase transitions of the first kind of goes into a curve of phase transitions of the second kind. In the vicinity of the critical point phase transitions of the first kind are similar to the second order phase transitions. Thermodynamic quantities that depend on the first derivative of thermodynamic potential: entropy, specific volume, and others have small jumps of these derivatives, with simultaneous anomalous behavior of thermodynamic quantities that depend on the second derivative of thermodynamic potential: heat capacity, isothermal compressibility, thermal expansion coefficient, and others.

Phase transitions and related critical phenomena, vastly complicate the problem of their investigation both as physically and as mathematically. From a physical point of view of the complexity of critical phenomena is reduced to the necessity of explicit taking account of statistical fluctuations in the vicinity of the phase transition. Their existence and anomalous large value leads to an anomalous features a number of thermodynamic quantities. All physical difficulties inevitably manifested in attempts to make correct mathematical description of critical phenomena. At creation of corresponding mathematical models are used phenomenological [16,17] and atomistic approaches [18,19]. MD models describe a collection

of interacting particles (atoms, ions, molecules), and represent a system of differential equations. When using the MD models for the investigation of various properties of materials, including to determine the critical parameters $p_{cr}, \rho_{cr}, T_{cr}$ crucial role played by the choice of the interaction potentials between particles, since the accuracy of the results is directly dependent on it.

Therefore, despite the wide opportunities of MD models, their usage requires a careful test calculations to determine the suitability of the selected interaction potentials in certain specific circumstances. This problem is especially acute in material with covalent bonds, which include silicon.

Interatomic interaction in silicon is more complicated than in metals. Silicon refers to materials with covalent binding and has a number of structural features. So, under normal conditions, the silicon has a diamond structure, characterized by a small compactedness with the coordinate number of 4, which is much less than that of metals (8-12). As the pressure increases in silicon formed new structures - simple cubic, face-centered cubic with increasing coordination number, but differ little in energy. After melting liquid silicon becomes a metal with a coordination number of about 6 and with density greater than the density of the solid phase. The presence of these features makes the problem of constructing the interatomic interaction potential for silicon is not a simple task. At present there are several approaches to the construction of interatomic potentials for materials with covalent bonds. The best known and frequently used are the potentials Stillinger-Weber, (SW) [20], modification of Stillinger-Weber (SWM) [21], Tersoff, (T-C, T-D) [22 - 24], Erhart-Albe, (EA -1, EA-2) [25, 26] and KIHS [27], EDIP [28-30]. Comparative analysis of interatomic interaction potentials for crystalline silicon, made in [31] shows that in the aggregate of mechanical and thermophysical parameters and characteristics the results of calculations with any of the potential does not satisfy the required accuracy of coincidence with the referenced and experimental data. The smallest number of poorly matching parameters and characteristics in a wide range of temperature and pressure for monocrystalline silicon has showed by potentials SW, KIHS, EA-2 and MIX (MIX = (31KIHS + SWM)/32) - a linear combination of two potentials: SWM and KIHS). This fact should be taken into account when determining the parameters of the critical point. Therefore, by analogy with [31] simulation was carried out with the same interaction potentials, supplemented potential MIX [31]. Comparison of simulation results among themselves, with the experimental estimates and calculations of other authors will allow to estimate in the aggregate of characteristics the most appropriate interaction potential suitable for describing processes in the near-critical region.

To determine the critical parameters, there are several methods: of saturated vapor, of the heat of vaporization and of the average cluster size in the critical region, as well as meniscus, Cailletet - Mathias and isotherms methods (Van der Waals criteria) [7, 9, 32,33] that never used together and did not analyzed for their applicability. Statement of computational experiment allows for all of these methods to perform research for a wide class of interaction potentials on a single methodological basis and from a comparative analysis of simulation results to determine the most reliable values of the critical parameters of silicon.

3 STATEMENT OF THE PROBLEM, MATHEMATICAL MODEL AND COMPUTATIONAL ALGORITHM

Mathematical model. The basis of the method of molecular dynamics (MD) is a model representation of a multi-atomic molecular system in which the particles are represented by material points, each of which has a mass, radius vector and velocity, respectively $m_i, \vec{r}_i, \vec{\upsilon}_i$, where $i = 1 \ldots N$. Interaction between the particles is carried out by forces $\vec{F}_i = -\frac{\partial U(\vec{r}_1 \ldots \vec{r}_N)}{\partial \vec{r}_i}$, where $U(\vec{r}_1 \ldots \vec{r}_N)$ is the potential energy of interaction of the system of N particles; interaction with the external field occurs through the of force $\vec{F}_i^{ext}$. In the classical case, the movement of an ensemble of particles is described by the Newton equations.

As a result, the mathematical formulation of the problem consists of a system of ordinary differential equations, their difference analogue (difference scheme), the interatomic interaction potential and specifically defined initial and boundary conditions. The evolution of an ensemble of particles is described by the system of 2N ordinary differential equations of motion:

$$\begin{cases} m_i \dfrac{d\vec{\upsilon}_i}{dt} = \vec{F}_i + \vec{F}_i^{ext} \\ \dfrac{d\vec{r}_i}{dt} = \vec{\upsilon}_i \qquad i = 1 \ldots N \end{cases} \tag{1}$$

Initial conditions. Integration of the system of equations (1) requires the knowledge of the coordinates and velocities $(\vec{r}_i, \vec{\upsilon}_i)\big|_{t=0}$ for all N particles at the initial time t=0. At the initial time, the simulated environment is a crystal, polycrystal or liquid. To specify the initial values of macroscopic parameters more accurately as well as to ensure the sustainability of the system, a relaxation of the simulated ensemble is performed after setting the coordinates and velocities.

Combined use of a thermostat and barostat that returns energy to the chaotic component of the particle motion to hold a given temperature T and pressure allows to quickly bring the system to a steady state. After bringing the system to such state, certain modified values of the lattice constant, taking into account the influence of the boundaries of the object will be reached automatically.

Boundary conditions. In the case of an infinite domain with respect to one, two or three spatial directions *X, Y, Z*, the modeling of the processes is performed in the finite computational domain with the dimensions $L_x \times L_y \times L_z$ along *X*, *Y*, *Z* axes correspondingly. Periodic boundary conditions are used along *X*, *Y*, *Z* axes with the periods of L_x, L_y, L_z correspondingly.

Periodic boundary conditions along *X* assume that the particles with the coordinate *x* within the range of $0 \le x < L_x$ exactly represent the particles within $kL_x \le x < (k+1)L_x$ for any

integer $k \neq 0$. That is, the particle leaving the computational domain from the upper boundary $x = L_x$ is replaced by a new particle with the same value of velocity but entering the computational domain from the bottom boundary $x = 0$. If the accent marks the quantities relating to the new particle then:

$$\begin{cases} \vec{\upsilon}' = \vec{\upsilon} \\ x' = (x - L_x) \ \in \ [0, L_x) \ \text{for} \ L_x \le x < 2L_x \\ y' = y \\ z' = z \end{cases}$$

Similarly, for particles leaving the computational domain through the lower boundary $x = 0$:

$$\begin{cases} \vec{\upsilon}' = \vec{\upsilon} \\ x' = (x + L_x) \ \in \ [0, L_x) \ \text{for} \ -L_x \le x < 0 \\ y' = y \\ z' = z \end{cases}$$

The second important aspect of periodic boundary conditions is the force and potential energy of interaction of particles from the boundary areas: $0 \le x < r_{cr}$ and $(L_x - r_{cr}) \le x < L_x$, where r_{cr} is the cutoff radius for the potential (it is assumed that one can neglect the forces at the distances $r > r_{cr}$).

Interaction of the particle i, which coordinate x_i is within the range of $(L_x - r_{cr}) \le x_i < L_x$, with the particles beyond the computational domain $L_x \le x'_j < (L_x + r_{cr})$, is modelled using the particles $0 \le x_j < r_{cr}$ from the computational domain with radius-vectors being corrected during calculating the force $\vec{F}_{ij} = \vec{F}_{(\ldots \vec{r}'_j \ldots)}(\vec{r}_i)$ in the following way:

$$\vec{r}'_j = \vec{r}_j + \vec{e}_x L_x \ ,$$

where $\vec{e}_x$ is the axis X unit vector.

Obviously, all of the above applies equally to the periodic boundary conditions along the coordinate axes Y and Z.

Computational algorithm. As the object of the study we chose a dielectric film with the thickness of Z = 32 nm along the primary axis and with total size of the computational domain of 268 nm along that axis. The particles of the vapor phase were removed from the computation upon reaching the boundaries (permeable reflectionless boundaries). The size of the computational domain was 8x8 nm along the axes X, Y, with periodic boundary conditions. The total initial number of particles was 96 000. The mass of the particles corresponded to the one of silicon. The computations were performed for Si (diamond lattice with the lattice constant of 5.43A) with periodic boundary conditions (3D problem). The

integration timestep was set to 2 fs.

The computational algorithm was based on the finite-difference Verlet scheme [34]. During modeling we used different statistical ensembles: the microcanonical ensemble (NVE), where the number of particles N, the volume V and the total energy E are constant, the canonical ensemble (NVT), where only the kinetic energy of the molecules (temperature) is fixed instead of the total energy, and isothermal-isobaric ensemble (NPT), which provides a constant pressure. The velocity (for NVT) and pressure (for NPT) adjustment was carried out by means of a thermostat and Berendsen barostat.

A more detailed description of the mathematical statement of the problem and its numerical realization can be found in [35],[36].

4 MODELING RESULTS, DISCUSSION

We used the following approaches to determine the parameters of the critical point.

a) Method of the meniscus [9].

This method allows determining in a clear way the range of temperatures and densities, where the critical point is located for each of the considered interaction potentials. The method is based on the direct observation of the liquid and vapor in the two phase system in the numerical experiment.

The computational domain is partially filled with the model liquid at the temperature knowingly below the critical point. In a series of experiments, the initial temperature was set to 4000K. The initial mass of liquid m_{liq} was set low enough so that the average density calculated as the relation of this mass to the total volume of the computational domain m_{liq}/V was certainly below the critical density. Next, the system is brought to a steady state, in which a dynamic equilibrium is set between the liquid and the saturated vapor when the flow of particles emitted from the fluid is equal to the flow of particles returning from the vapor to the liquid. This is the state when the values of the pressure as well as the values of the density of liquid and saturated vapor are measured in the system.

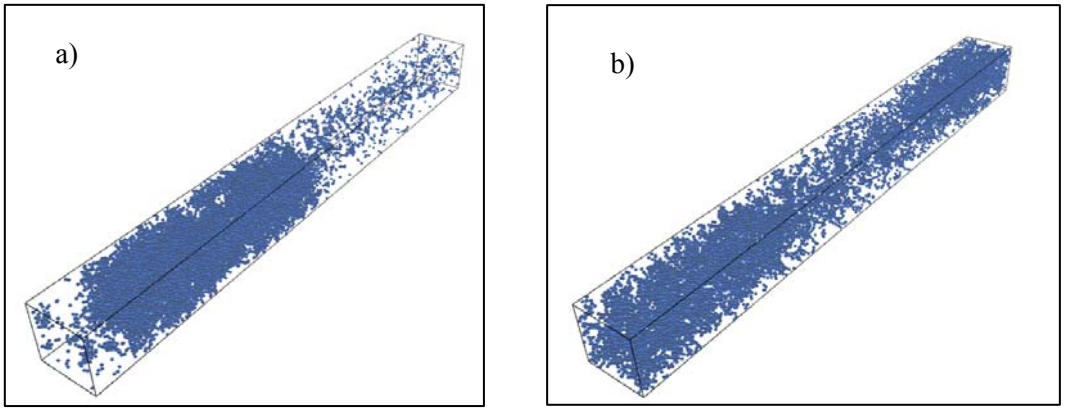

Fig.1. Steady states in the computational domain at 7000 K (a) and 8000 K (b) for the potential T-C.

This experiment and measurements are repeated at every step at the higher temperature

value. At some temperature value of T_0, the density becomes uniform across the whole computational domain. Fig. 1 shows an example of two steady states for the non-uniform (a) and uniform (b) distributions of density across the volume at the temperatures of 7000 K и 8000 K correspondingly. Since the initial mass of liquid was such that the average density was certainly below critical one, then $T_0 < T_{cr}$ as well, i.e. at such temperature the liquid will vaporize completely.

Then the initial mass of liquid (at constant size of the computational domain) is increased and a series of experiments with different temperatures is repeated again. The temperature T_0 is determined again, i.e. when the density becomes uniform across the volume of the computational domain for the new initial mass of liquid m_{liq}. The dependence $T_0(m_{liq})$ is non-monotonous and has a maximum equal to the critical temperature T_{cr} exactly when $m_{liq}/V = \rho_{cr}$. To clarify the position of this peak, we further use the method of Cailletet-Mathias [7]. Thus, the critical parameters are in the region of the transition from a state in which one can clearly distinguish the boundary between liquid and vapor (lower limit) to a state where the entire system is uniformly occupied with vapor (upper limit).

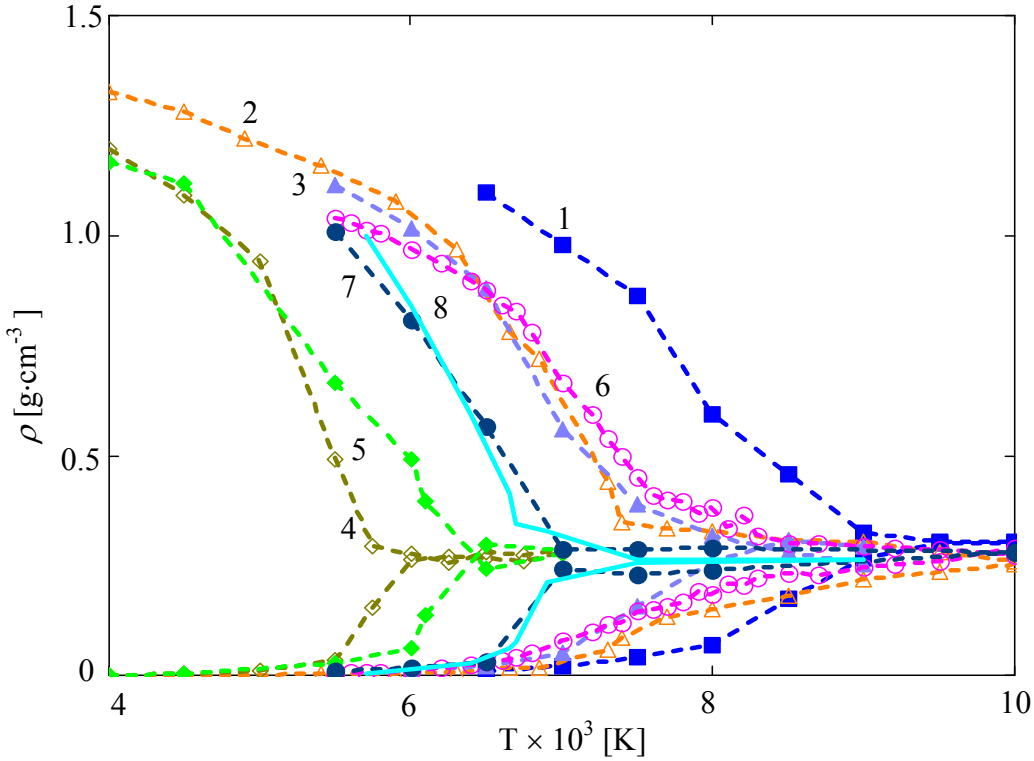

1 – SW; 2 – T-C; 3 – T-D; 4 – EA-1; 5 – EA-2; 6 – EDIP; 7 – KIHS; 8 – MIX.

Fig.2. Temperature dependence of the saturated vapor (below) and liquid (above) for different potentials.

b) Method of Cailletet and Mathias [7].

According to this method, the average density of the liquid and gaseous phases lie on a straight line, called the rectilinear diameter. The point of intersection of the rectilinear diameter with the density curve determines the critical value of the density and temperature.

Fig. 2 shows the temperature dependence of the densities of the liquid and vapor, resulting from a series of experiments described above, which are used to clarify the critical parameters using this method.

Thus, we used here the definition of the critical temperature as the temperature, at which the pressure and density of the vapor have a maximum, while the density of the liquid being in a dynamic equilibrium with the vapor is minimized.

c) Temperature dependence of the saturated vapor [7].

One can determine the critical pressure (at the known critical temperature) analyzing the temperature dependence of the pressure of the saturated vapor. The obtained temperature dependencies of the saturated vapor pressure are shown in Fig. 3. When passing through the critical point, there is a change of behavior: the strongly non-ideal saturated vapor described by an exponential function in the subcritical region is transformed into an ideal one with the linear dependence in the supercritical region.

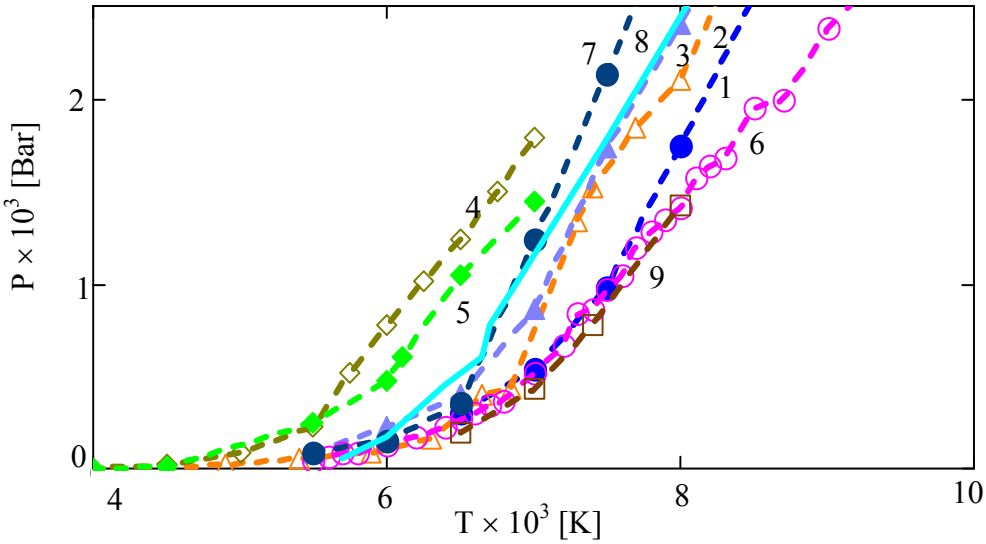

1 – SW; 2 – T-C; 3 – T-D; 4 – EA-1; 5 – EA-2; 6 – EDIP; 7 – KIHS; 8 – MIX; 9 – SWM.

Fig. 3. Temperature dependencies of the saturated vapor pressure for different potentials

d) Temperature dependence of the heat of vaporization [33].

Since in the critical point the dividing line between the properties of the gaseous and liquid phases disappears, the heat of vaporization, which is determined by the difference of the enthalpies of the liquid and gaseous phases, vanishes. In a series of computational experiments similar to those described above, the temperature dependencies of the enthalpy of the liquid phase and the vapor were measured. Next, we calculated the difference between them at the same temperatures and obtained a family of curves for different interaction potentials (Fig. 4). The point where the heat of vaporization vanishes was assumed as the critical temperature for each of the potentials used.

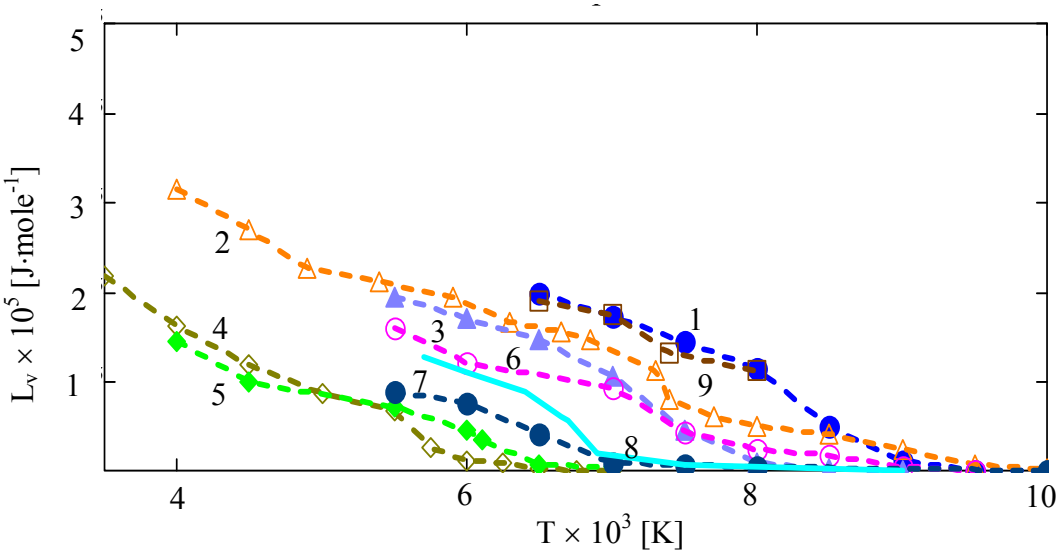

1 – SW; 2 – T-C; 3 – T-D; 4 – EA-1; 5 – EA-2; 6 – EDIP; 7 – KIHS; 8 – MIX; 9 – SWM.

Fig.4. Temperature dependence of evaporation heat

e) Temperature dependence of the average cluster size.

In the subcritical region, the density and pressure of saturated vapor increase with increasing temperature. In the near-critical region, atomic vapor particles begin to unite into clusters, which reach their maximum size just at the critical point. As the temperature increases further, the density no longer grows. In this case, the clusters begin to break up into smaller ones due to the increase of the kinetic energy of random motion. That is, the average size of the cluster must have a singularity at the critical point. This fact is used in this method to determine the critical temperature.

Mean number of atomic particles forming a cluster can be estimated using the formula

$$\langle N \rangle = \frac{n(T) k_B T}{P_{sat}(T)},$$

where $P_{sat}(T)$ is the saturated vapor pressure at the temperature T, $n(T)$ is the concentration of atomic particles in the saturated vapor.

The temperature dependence of $\langle N \rangle$ temperature has a typical bend at the critical point (Fig.5).

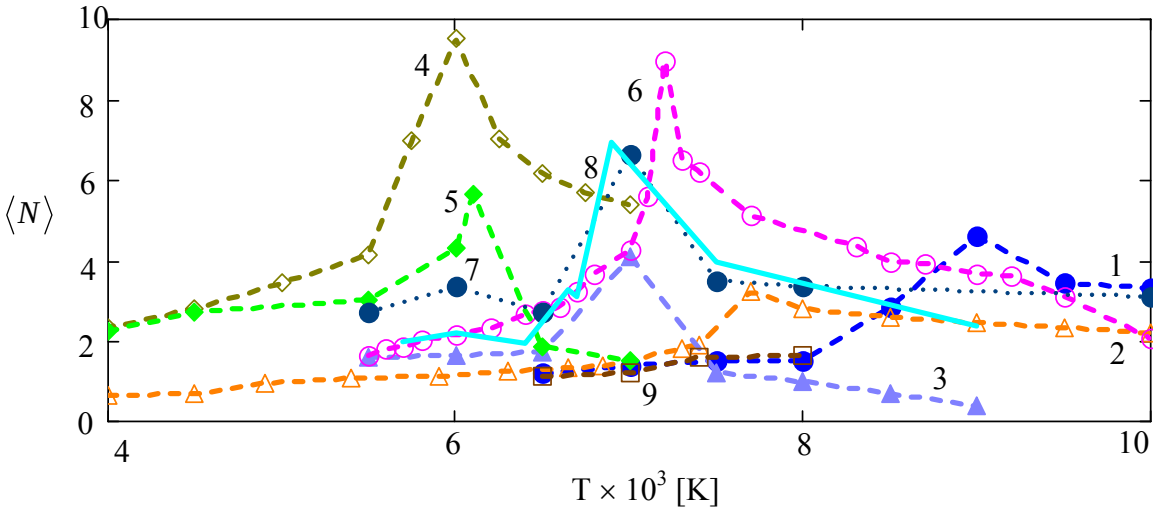

1 – SW; 2 – T-C; 3 – T-D; 4 – EA-1; 5 – EA-2; 6 – EDIP; 7 – KIHS; 8 – MIX; 9 – SWM.

Fig.5. Temperature dependence of the average cluster size

f) Method of isotherms (criteria of Van der Waals) [7,9].

It is known from the theory of van der Waals that in the critical point, the first and second derivatives of the pressure with regard to volume (density) vanish. For a set of fixed values of temperature (in the range of sub- and super-critical values), the dependencies (isotherms) of pressure vs. density for each of the potentials are plotted. To do this, a cubic computational domain with periodic boundary conditions in all three axes is completely filled with liquid at a fixed temperature. The system is brought to a steady state and then the pressure is measured. Further, the size of the computational domain without changing the number of particles and keeping the temperature constant is increased in the same three directions. Again, the system relaxes to a steady state and the pressure is measured.

Since the isotherms corresponding to a temperature below the critical one have a deflection and a clear minimum, one can select the isotherm, in which the deflection and minimum are absent (tangent to the graph is zero) - and it will be the closest to the critical isotherm. For example, for the potential of Erhart-Albe2 at T=5500 K, the isotherm has a clear deflection (Fig. 6). For the isotherm T=6250 K, it is almost imperceptible.

Received critical parameters of silicon (Fig. 1-6) are summarized in Table 1. Estimates of the parameters of the critical point [37, 38] used in the industry as well as the results of a simulation performed by the authors [39,40] Monte Carlo for a potential Stillenzhera - Weber placed there as well.

Critical temperature determined from the dependence (Fig. 1-6). The procedure for calculating the average cluster size was the most accurate. The critical pressure is determined from the temperature dependence of the saturated vapor, Fig. 3. Cailletet - Mathias method for determining the values of the critical density was used.

If the basis is recommended estimations [37, 38], the potentials of the EA-1, EA-2, KIHS and MIX show closest values of the critical parameters. Potentials WS and Tersoff show the largest deviation from the recommended estimations [37, 38].

At the same time the critical parameters for the potential Stillinger-Weber is in good agreement with the results for the SW obtained in the calculation [39, 40], which indicates that the decisive role of the interaction potential, rather than the method that was used.

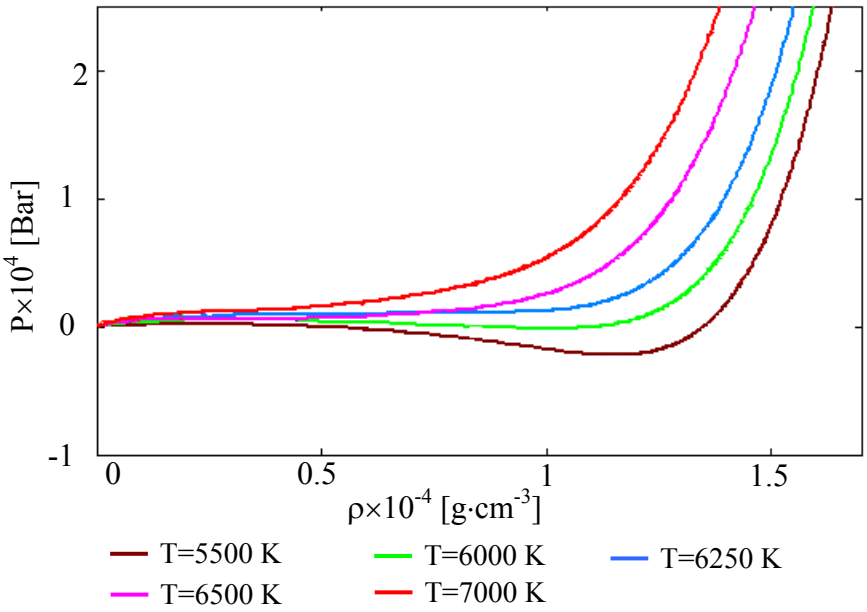

Fig.6. Method of isotherms to determine the critical temperature (potential of EA-2).

	Critical temperature, K	Critical density, g/cm^3	Critical pressure, bar
SW [20]	8550 ± 250	0.27 ± 0.06	2200 ± 400
T-C [23]	7750 ± 250	0.24 ± 0.04	1900 ± 100
EDIP [29]	7500 ± 250	0.31 ± 0.08	1000 ± 100
T-D [24]	7250 ± 250	0.23 ± 0.07	1300 ± 300
SWM [21]	7700 ± 250	0.25 ± 0.06	1200 ± 200
KIHS [27]	6850 ± 250	0.24 ± 0.06	800 ± 300
MIX [31]	6650 ± 250	0.22 ± 0.07	650 ± 100
EA-1 [26]	5750 ± 250	0.19 ± 0.05	500 ± 100
EA-2 [25]	6250 ± 250	0.24 ± 0.04	800 ± 100
Estimations [37, 38]	5160	0.1207	530
Calculations (SW) [39]	7500 ± 500	0.75 ± 0.1	-
Calculations (SW) [40]	7925 ± 250	0.76 ± 0.5	1850 ± 400

Table. 1. Critical parameters of silicon for different interaction potentials.

5 CONCLUSIONS

According to carried out computational experiments and analysis of the dependencies were determined critical values: pressure p_{cr}, density ρ_{cr} and temperature T_{cr} of the silicon to 9 interaction potentials. Statement of computational experiments carried out for 6 physical methods: meniscus [9], Cailletet - Mathias [7], the van der Waals isotherms [7,9], the temperature dependence of the saturated vapor [7], the temperature dependence of the heat of vaporization [33] and the average cluster size (method proposed by the authors).

Comparison of the simulation results (Table 1) with critical parameters used in practical applications [37,38] showed that the best agreement observed for potentials EA-1, EA-2, MIX and KIHS.

Comparison of the obtained critical parameters for the potential Stillinger -Weber [20] with results of calculations based on Monte-Karlo methods [39,40] for the same potential showed good agreement of results with each other, but with a large scatter of data [37,38]. Performed analysis allows us to recommend for modeling high-temperature processes ($T_m < T \le T_{cr}$) in silicon exactly potentials EA-1, EA-2, MIX and KIHS, in contrast to low-temperature processes ($T \le T_m$) where according to [31] classical potential Stillinger -Weber [20] and potentials KIHS, EA-2 and MIX have the advantage.

This work was supported by RFBR projects №13-07-00597, №15-07-05025.

REFERENCES

[1] Shang-Keng Ma, *Modern Theory of Critical Phenomena,* Benjamin, New York, (1976). Perseus, (2000).

[2] H. E. Stanley, *Introduction to Phase Transitions and Critical Phenomena,* Oxford University Press, Oxford and New York, (1971).

[3] Zel'dovich Ya B and Raizer Yu P, *Physics of Shock Waves and High-Temperature Hydrodynamic Phenomena*, New York: Academic, (1966).

[4] *Shock waves and extreme states of matter*, Under. Ed. V.E.Fortova, L.V.Altshulera et al., Moscow, Nauka, (2000).

[5] Soboleva E.B., "On the influence of the equation of state for simulation of convective flow and heat transfer in the near-critical fluids", *Teplofizika vysokikh temperature*, **38**, 6, 928 - 934, (2000).

[6] Povarnitsyn M.E, Itina T. E, Levashov P. R., Khishchenko K. V., "Simulation of ultrashort double-pulse laser ablation", *Applied Surface Science*, **257,** 5168–5171, (2011).

[7] V.A. Kirililin, V.V. Sychev, A.E. Sheindlin, *Technical thermodynamics*, M.: Izdatel`stvo MEI, (2008).

[8] Skripov V.P., *Metastable liquid,* M., Nauka, (1972).

[9] Leibfrid G., *Microscopic theory of mechanical and thermal properties of crystals*, M.: Fizmatgiz, (1963).

[10] Shambhu N. Sharma, Hiren G. Patel, *The Fokker-Planck equation. Stochastic Control*, Edited by Chris Myers, ISBN 978-953-307-121-3, Publisher Sciyo, Published in print edition August, InTech, (2010).

[11] Fortov V.E., Dremin A.N., Leont`ev A.A., "Estimation of the parameters of the critical point", *Teplofizika vysokikh temperature*, **13**, 5, 1072-1079, (1975).

[12] V.E.Fortov, I.V.Lomonosov, "Ia.B. Zeldovich and problems of equations of state of matter under extreme conditions", *UFN*, **184**, 3, 231 – 245, (2014).

[13] Morel V, Bultel A, Cheron B G., "The Critical Temperature of Aluminum", *Int. J. Thermophys*, **30**, 1853-1863, (2009).

[14] Porneala C, Willis D.A., "Time-resolved dynamics of nanosecond laser-induced phase explosion", *J. Phys. D: Appl. Phys*, **42**, 155503 (1-8) (2009).

[15] C.Wu, L.V. Zhigilei, "Microscopic mechanisms of laser spallation and ablation of metal targets from large-scale molecular dynamics simulations", *Appl. Phys. A*, **114**, 11-32, (2014).

[16] Lu Q., Mao S.S., Mao X., Russo R. E., "Delayed phase explosion during high-power nanosecond laser ablation of silicon", *Applied Physics Letters*, **80**, 17, 3072-3074, (2002).

[17] D. Autrique, G. Clair, D. L'Hermite, V. Alexiades, A. Bogaerts, B. Rethfeld, "The role of mass removal mechanisms in the onset of ns-laser induced plasma formation", *J.Appl. Phys.*, **114**, 023301 (1-10), (2013).

[18] Perez D, Lewis L.J., "Molecular-dynamics study of ablation of solids under femtosecond laser pulses", *Phys. Rev. B*, **67**, 184102 (1 –15), (2003).

[19] Cheng J., Liu C., Shang S., Liu D., Perrie W., Dearden G., Watkins K., "A review of ultrafast laser materials micromachining", *Optics & Laser Technology*, **46,** 88–102, (2013).

[20] H. Stillinger and T. A. Weber, "Computer simulation of local order in condensed phases of silicon", *Phys. Rev. B*, **31**, 5262-5271 (1985).

[21] L. Pizzagalli, J. Godet, J. Guenole, S. Brochard, E. Holmstrom, K. Nordlung, T. Albaret, "A new parameterization of the Stillinger-Weber potential for an improved description of defects and plasticity of silicon", *J. Phys, Condens. Matter* **25**, 055801, (2013).

[22] J. Tersoff, "New empirical model for the structural properties of silicon", *Phys. Rev. Lett.* **56**, 632-635 (1986).

[23] J. Tersoff, "New empirical approach for the structure and energy of covalent systems", *Phys. Rev. B*, **37**, 6991-7000, (1988).

[24] J. Tersoff, "Modeling solid-state chemistry: Interatomic potentials for multicomponent systems", *Phys. Rev. B,* **39**, 5566-5568, (1989).

[25] P. Erhart and K. Albe, "The role of thermostats in modeling vapor phase condensation of silicon nanoparticles", *Appl. Surf. Sci*., **226**, 12-18, (2004).

[26] P. Erhart and K. Albe, "Analytical potential for atomistic simulations of silicon, carbon, and silicon carbide", *Phys. Rev. B,* **71**, 035-211 (2005).

[27] T. Kumagai, S. Izumi, S. Hara, and S. Sakai, "Development of bond-order potentials that can reproduce the elastic constants and melting point of silicon for classical molecular dynamics simulation", *Comp. Mater. Sci*. **39**, 457, (2007).

[28] M. Z. Bazant, E. Kaxiras, "Modeling of covalent bonding in solids by inversion of cohesive energy curves", *Phys. Rev. Lett.* **77**, 4370 (1996).

[29] M. Z. Bazant, E. Kaxiras, J. F. Justo, "Environment-dependent interatomic potential for bulk silicon", *Phys. Rev. B*, **56**, 8542, (1997).

[30] J. F. Justo, M. Z. Bazant, E. Kaxiras, V. V. Bulatov, and S. Yip, "Interatomic potential for silicon defects and disordered phases", *Phys. Rev. B*, **58**, 2539 (1998).

[31] Mazhukin V. I., Shapranov A. V., Rudenko A. V., "Comparative analysis of potentials of interatomic interaction for crystalline silicon", *Mathematica Montisnigri*, **30**, 56-75, (2014).

[32] Kireev V.A. Short, *Course of Physical Chemistry*, M., (1970).

[33] J. O. Hirschfelder, Chf. Curtiss, R. B. Bird, *Molecular theory of gases and liquids*, Wiley, New York, (1954).

[34] Verlet L., "Computer "Experiments" on Classical Fluids. I. Thermodynamically Properties of Lennard-Jones Molecules." *Phys. Rev*., **159**, 98-103, (1967).

[35] Mazhukin V.I., Shapranov A.V., Samokhin A.A., Mazhukin A.V. Koroleva O.N., "Visualization and analysis of the results of molecular-dynamic modeling of intensive evaporation of liquid in the near-critical region", *Scientific Visualization,* **6**, 4, 72-95, (2014).

[36] Mazhukin V.I., Shapranov A.V., Samokhin A.A., Ivochkin A.Yu., "Mathematical modeling of non-equilibrium phase transition in rapidly heated thin liquid film", *Mathematica Montisnigri*, **27**, 65 - 90, (2013).

[37] *Innovative Engineering with Advanced Material Science*, SiFusion Polysilicon Furnaceware Technology, http://sifusion.ferrotec.com/products/sifusion/science/physical/.

[38] *Physical Properties and Critical Constants of Silicon*, Boston Electronics Corporation, http://www.boselec.com/products/matsiphy.html.

[39] N. Honda, Y. Nagasaka, "Vapour-liquid equilibrium of Silicon by Gibbs Ensemble Simulation", *Int. J. Thermophys*, **20**, 837 - 846, (1999).

[40] D. V. Makhov, Laurent J. Lewis, "Isotherms for the liquid-gas phase transition in silicon from NPT Monte Carlo simulations", *Phys. Rev. B*, **67**, 153202, (2003).

Received February, 10 2014